Engineering of the passband function of a generalized spectrometer

J.D. McKinney and A.M. Weiner

Purdue University, School of Electrical and Computer Engineering
465 Northwestern Avenue, West Lafayette, IN 47907-2035

mckinnjd@purdue.edu

Abstract: To our knowledge, we demonstrate a new scheme for passband engineering of a grating spectrometer. Through spatial masking of the input beam and translation of the optical components we present shaping, shifting, and scaling of the passband in optical frequency. Specifically, we demonstrate the relationship between the applied spatial masking function and the spectrometer passband may be tuned from an exact Fourier transform to a direct scaling through longitudinal displacement of the spectrometer lens and sampling slit and that this operation is independent of the choice of spectrometer center frequency.

OCIS codes: 120.6200 Spectrometers and spectroscopic instrumentation, 320.5540 Pulse shaping

References and links

1. F. Kneubuhl, "Diffraction Grating Spectroscopy," Appl. Opt. **8**, 505–519 (1969).
2. D. E. Leaird and A. M. Weiner, "Femtosecond direct space-to-time pulse shaping," IEEE J. Quantum Electron. **37**, 494–504 (2001).
3. J. D. McKinney and A. M. Weiner, "Direct Space-to-Time Pulse Shaping at 1.5 μm," IEEE J. Quantum Electron. **39**, 1635–1644 (2003).
4. D. E. Leaird and A. M. Weiner, "Femtosecond optical packet generation by a direct space-to-time pulse shaper," Opt. Lett. **24**, 853–855 (1999).
5. J. D. McKinney, D. S. Seo, D. E. Leaird, and A. M. Weiner, "Photonically Assisted Generation of Arbitrary Millimeter-wave and Microwave Electromagnetic Waveforms via Direct Space-to-Time Optical Pulse Shaping," J. Lightwave Technol. **21**, 3020–3028 (2003).
6. H. O. Edwards and J. P. Daikin, "Gas Sensors using Correlation Spectroscopy Compatible with Fibre-optic Operation," Sensors and Actuators B **11**, 9–19 (1993).
7. M. B. Sinclair, M. A. Butler, S. H. Kravitz, W. J. Zubrzycki, and A. J. Ricco, "Synthetic Infrared Spectra," Opt. Lett. **22**, 1036–1038 (1997).
8. M. B. Sinclair, M. A. Butler, A. J. Ricco, and S. D. Senturia, "Synthetic Spectra: a Tool for Correlation Spectroscopy," Appl. Opt. **36**, 3342–3348 (1997).
9. D. E. Leaird and A. M. Weiner, "Chirp control in the direct space-to-time pulse shaper," Opt. Lett. **25**, 850–852 (2000).
10. J. W. Goodman, *Introduction to Fourier Optics*, 2nd ed. (The McGraw-Hill Companies, Inc., New York, 1996).
11. O. E. Martinez, "Grating and prism compressors in the case of finite beam size," J. Opt. Soc. Am. B **3**, 929–934 (1986).
12. E. Hecht, *Optics*, 2nd ed. (Addison-Wesley, Reading, 1987).
13. A. E. Siegman, *Lasers* (University Science Books, Sausalito, 1986).
14. A. Papoulis, "Pulse Compression, Fiber Communications, and Diffraction: A Unified Approach," J. Opt. Soc. Am. A **11**, 3–13 (1994).
15. A. M. Weiner, "Femtosecond pulse shaping using spatial light modulators," Rev. Sci. Instrum. **71**, 1929 (2000).
16. J. N. Mait, "Design of binary-phase and multiphase fourier gratings for array generation," J. Opt. Soc. Am. A **7**, 1514–1528 (1990).
17. M. Shirasaki, "Large Angular Dispersion by a Virtually Imaged Phased Array and Its Application to a Wavelength Demultiplexer," Opt. Lett. **21**, 366–368 (1996).

#5072 - $15.00 US Received 17 August 2004; revised 27 September 2004; accepted 1 October 2004

18. S. Xiao, A. M. Weiner, and C. Lin, "A Dispersion Law for Virtually Imaged Phased-Array Spectral Dispersers Based on Paraxial Wave Theory," IEEE J. Quantum Electron. **40**, 420–426 (2004).

1. Introduction

Despite the widespread use of diffraction grating-based spectrometers [1], surprising new behavior is found to arise in even the simplest of these devices. In this work we demonstrate essentially new opportunities for engineering the spectrometer passband function of a simple spectrometer. Specifically, we demonstrate that spatial masking of the input beam allows synthesis of highly-structured passband functions that may be scaled and shifted in optical frequency through simple translation of the spectrometer components.

The temporal behavior of the grating spectrometer with a spatially patterned input has been well analyzed in the context of direct space-to-time (DST) pulse shaping [2, 3]. This pulse shaping technique - which relies on the direct mapping of an applied spatial input pattern to the output temporal waveform - has been applied to generation of high-rate optical pulse sequences [4] as well as combined with high-speed optical-to-electrical conversion to generate arbitrary millimeter and microwave waveforms [5].

The spectral capabilities of the apparatus, which is essentially a grating-lens-slit spectrometer with a spatially patterned input beam, have remained largely unexplored until now. Some of the spectral properties of the apparatus, specifically the ability to control the center wavelength of the output spectrum and the relation of the output spectral shape to the input spatial masking function, were analyzed in [2]. This work demonstrated that the spectrometer passband function (and, hence, the shape of the output spectrum) was related to the Fourier transform of the applied spatial masking function (and output temporal waveform) and that the center wavelength of the output spectrum could be selected via the transverse position of the output slit. In time-domain applications, this means that multiple output pulse sequences - each with a different center wavelength - could be generated from a single DST pulse shaper. In this work, we focus on the frequency-domain behavior of the apparatus. We show here, for the first time to our knowledge, that the spectrometer passband function may be tailored through direct manipulation of the input spatial masking function through space-to-wavelength mapping.

We expect the ability to tailor the passband function of such a generalized spectrometer will have significant future impact on the field of correlation spectroscopy [6]. This technique is based on correlating a known reference spectrum (either absorption or emission) with that of an unknown compound. The resulting frequency-dependent correlation function then provides information on whether the unknown compound corresponds to the reference. Typically, a broadband optical input beam passes through both the reference and unknown sample cells and the overall transmission through both is measured with an infra-red detector. The ability to shape the output spectrum from our apparatus provides a straightforward method for generating the requisite reference spectrum for these systems. In contrast to diffractive optical element-based approaches [7, 8], our passband functions (reference spectra) may be shifted and scaled without the need to change the input masking function or observation angle. In addition, our system may be easily altered for two-dimensional operation through the use of 2-D spatial light modulators. This would allow arrays of passband functions to be generated simultaneously, enabling correlation processing against multiple reference spectra at the same time. One can envision additional applications in broadband spectral imaging, as well as ultrafast optical signal processing.

Our paper is organized as follows. In Section 2 we will discuss the operation of the generalized spectrometer from a mathematical point of view. Specifically, in 2.1 we will analyze the perfectly aligned ($f - f$ configuration) from a Fourier optics point of view. In 2.2 we will present a simple ray-tracing argument for the operation of the apparatus in the limit of large

#5072 - $15.00 US Received 17 August 2004; revised 27 September 2004; accepted 1 October 2004

lens displacements, followed by a more rigorous diffraction analysis. Section 3 will present experimental data showing both Fourier and direct passband engineering of the generalized spectrometer, and in Section 4 we will conclude.

2. Theory

Our work relies on the fact that the spectrum at the output of a spectrometer is given by the product of the input optical spectrum $E_{in}(\lambda)$ and a modified spatial Fourier transform of the applied spatial masking function $m(x')$ evaluated as a scaled function of optical wavelength. The latter of these is termed the spectrometer passband function and is the focus of this work. The following analysis treats the generalized spectrometer purely as a spectroscopic device, that is we place no requirements on the input optical source - such as assuming a short pulse - as the spectral properties of the device do not depend on the input source. It should be noted, however, that the spectral scaling properties presented here could alternatively be derived from the time-domain chirp analysis of the apparatus used as a DST pulse shaper [2, 9]. A schematic of our generalized spectrometer is shown in Fig. 1.

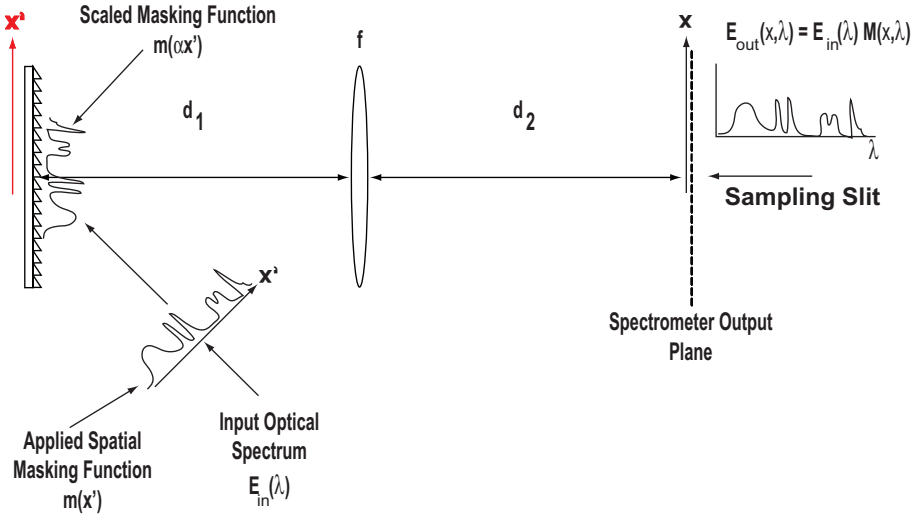

Fig. 1. Experimental setup. Our apparatus consists of a 600 l/mm diffraction grating, 150 mm achromat lens, and a singlemode fiber which functions as the output slit. In this work, the input spectrum $E_{in}(\lambda)$ is amplified spontaneous emission from an erbium doped fiber amplifier. The applied spatial masking function $m(x')$ is defined immediately before the diffraction grating.

2.1. *The perfectly aligned generalized spectrometer*

To begin the analysis, we consider the simple case of a spatial pattern $p(x')$ positioned in the front focal plane of a thin lens. When this spatial pattern is illuminated with a monochromatic plane wave, it is well known that the spatial field distribution in the back focal plane of the lens is given by the spatial Fourier transform $P(k_o x/f)$ of the spatial input pattern [10]. Mathematically,

$$E_{out}(x) = P\left(k_o \frac{x}{f}\right) \propto \int_{-\infty}^{\infty} dx'\, p(x') \exp\left(jk_o \frac{x}{f} x'\right), \tag{1}$$

#5072 - $15.00 US Received 17 August 2004; revised 27 September 2004; accepted 1 October 2004

where k_o is the freespace wavenumber

$$k_o = \frac{2\pi}{\lambda_o}, \tag{2}$$

x is the transverse coordinate in the output plane referenced to the optical axis, and $k_o x/f$ is the angular spatial frequency in m^{-1}. When the field illuminating the applied spatial pattern is polychromatic with amplitude spectrum $E_{in}(\lambda)$ (with a bandwidth much less than the center wavelength ($\Delta\lambda \ll \lambda_o$)), the field distribution in the output plane is given by

$$E_{out}(x,\lambda) \propto E_{in}(\lambda) \int_{-\infty}^{\infty} dx'\ p(x') exp\left(j\frac{k_o}{f}xx'\right). \tag{3}$$

When a diffraction grating is positioned in the front focal plane of the lens, spatial dispersion couples optical wavelength and spatial frequency in the back focal plane of the lens. Thus, for a user-defined masking function $m(x')$ defined immediately prior to the grating, the spatial pattern $p(x')$ in Eq. (3) becomes a scaled version of the masking function $m(x')$ multiplied by a frequency-dependent linear phase exponential

$$p(x') = m(\alpha x') exp\left[-jk_o(\lambda-\lambda_o)\frac{d\theta_D}{d\lambda}x'\right]. \tag{4}$$

Here, we assume linear spatial dispersion where

$$\frac{d\theta_D}{d\lambda} = \frac{1}{d\cos\theta_{D_o}}, \tag{5}$$

d is the pitch of the diffraction grating, and θ_{D_o} is the diffraction angle of the reference wavelength (λ_o). In addition to angular dispersion, the grating imparts a spatial scaling factor (astigmatism) given by [11]

$$\alpha = \frac{\cos\theta_i}{\cos\theta_{D_o}}. \tag{6}$$

As shown in Fig. 1, the coordinate x' is orthogonal to the input beam; for clarity in subsequent figures, we will illustrate this coordinate immediately to the left of the grating as shown in red. The field distribution in the back focal plane of the lens is now related to the user-defined masking function $m(x')$ through the modified Fourier transform relation

$$E_{out}(x,\lambda) \propto E_{in}(\lambda) \int_{-\infty}^{\infty} dx'\ m(\alpha x') exp\left\{j\frac{k_o}{f}\left[x - f(\lambda-\lambda_o)\frac{d\theta_D}{d\lambda}\right]x'\right\}. \tag{7}$$

If we perform the Fourier transform in Eq. (7), the field distribution in the back focal plane of the lens is now a coupled function of space and wavelength

$$E_{out}(x,\lambda) \propto E_{in}(\lambda) M\left\{\frac{k_o}{\alpha f}\left[x - f(\lambda-\lambda_o)\frac{d\theta_D}{d\lambda}\right]\right\}, \tag{8}$$

where $M\{\ldots\}$ is the Fourier transform of the spatial masking function $m(x')$. When the output spectrum given in Eq. (8) is sampled with a thin slit (taken here to be a spatial δ function) positioned at transverse location x_s in the output plane, we have

$$E_{out}(x_s,\lambda) \propto E_{in}(\lambda) M\left\{\frac{k_o}{\alpha f}\left[x - f(\lambda-\lambda_o)\frac{d\theta_D}{d\lambda}\right]\right\}\delta(x-x_s). \tag{9}$$

#5072 - $15.00 US Received 17 August 2004; revised 27 September 2004; accepted 1 October 2004

We see that $M\{\ldots\}$ gives the spectral passband function, with center wavelength $\lambda_s(x_s)$ determined by the transverse position of the thin slit according to

$$x_s \;=\; f\,[\lambda_s(x_s)-\lambda_o]\,\frac{d\theta_D}{d\lambda}. \tag{10}$$

Solving for $\lambda_s(x_s)$ we obtain

$$\lambda_s(x_s) \;=\; \lambda_o+\frac{x_s}{f}\left(\frac{d\theta_D}{d\lambda}\right)^{-1}. \tag{11}$$

We note that $\lambda_s(x_s=0)=\lambda_o$, i.e., the passband is centered at λ_o at the origin of the transverse coordinate ($x_s=0$) in the output plane. The measured optical spectrum then becomes the product of the input spectrum and the Fourier transform of the applied spatial masking function evaluated as a scaled function of wavelength about the passband center wavelength $\lambda_s(x_s)$ (where Eq. (5) is inserted for $d\theta_D/d\lambda$)

$$E_{out}\,(x_s,\lambda) \;\propto\; E_{in}\,(\lambda)\,M\left\{\frac{k_o}{\alpha}\left[\frac{\lambda_s(x_s)-\lambda}{d\cos\theta_{D_o}}\right]\right\}. \tag{12}$$

In this work, our goal is to describe control of the spectrometer passband function $M\{\ldots\}$. Because this quantity is independent of the input amplitude spectrum $E_{in}(\lambda)$, we will ignore the input spectrum in the rest of our analysis. Experimentally, this is equivalent to dividing the measured output spectrum by that of the input, providing a direct measurement of the passband function.

In this case of an $f-f$ configuration, the Fourier transform relation between the input spatial masking function $m(x')$ and the passband function $M(\lambda)$ is exact. To illustrate the system operation in this case, consider the simple ray-tracing picture of Fig. 2. Here, the input beam

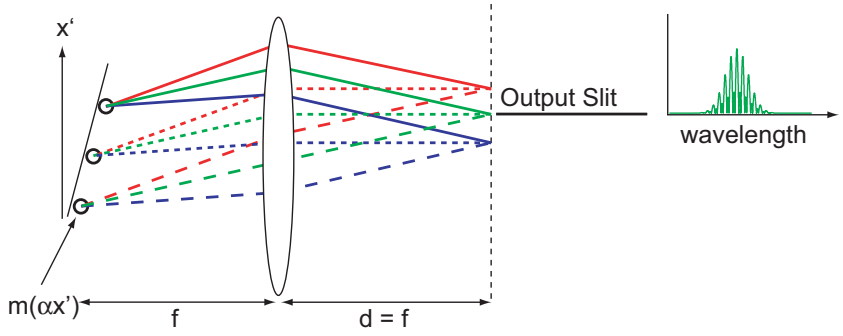

Fig. 2. A ray-tracing picture of the generalized spectrometer. When the apparatus is aligned in an $f-f$ configuration, the center wavelength of the output is chosen via the transverse position of the output slit and the shape of the optical spectrum is determined by the Fourier transform of the input spatial masking function. The colored lines represent the angular dispersion due to the diffraction grating.

is spatially patterned and applied to the diffraction grating. The spectral components from each feature at the grating are spatially dispersed and focused in the back focal plane of the lens. When the field in the output plane is sampled with a thin slit, the center frequency of the passband function is determined by the transverse slit position and the shape of the passband function with respect to wavelength is determined by the Fourier transform of the applied spatial

#5072 - $15.00 US Received 17 August 2004; revised 27 September 2004; accepted 1 October 2004

masking function. A simple way to view this is to look at the total field at the spectrometer output (Eq. (8)) as the sum of spatial Fourier transforms of the input masking function at slightly different wavelengths which are necessarily displaced from one another at the spectrometer output. Since the spatial extent of any one of these transforms is finite, a slit (even a spatial delta function) will sample a range of these spatial distributions. Given the wavelength dependent displacement, each distribution is sampled at a slightly different *apparent* spatial frequency which is a function of wavelength. So, the amplitude of given wavelength component is directly proportional to the amplitude at a specific *apparent* spatial frequency. In this process, the measured passband function takes the shape of the Fourier transform of the input spatial masking function. The actual optical bandwidth of the passband function in this case is relatively small, hence the monochromatic picture given in Fig. 2. As a note, when the input spectrum is coherent (i.e., that of a short pulse) the temporal output of the apparatus can be found by taking the inverse Fourier transform of the output spectrum of Eq. (12) with respect to optical frequency. In this case, the temporal output is the convolution of the short pulse input with a scaled version of the applied spatial masking function evaluated as a function of time, and the apparatus functions as a direct space-to-time pulse shaper [2, 3].

2.2. The generalized spectrometer in the limit of large lens displacements

When the apparatus is aligned such that the grating-lens and lens-slit separations are not equal to the focal length of the spectrometer lens, the behavior of the system changes dramatically. In the limit of large lens displacements, what occurs is that the shape of the input masking function is mapped onto the optical spectrum at the output of the spectrometer. This result may be obtained through a diffraction analysis of the system and this will, in fact, be treated towards the end of this section where we will also define the limit of large displacements. For now, we appeal to a simple and physically equivalent ray-tracing picture of the system operation to gain a physical idea of how this mapping from space-to-wavelength occurs.

To illustrate the behavior of the apparatus, we look at the case where the lens-grating distance (d_1 in Fig. 1) is equal to the focal length f of the spectrometer lens and observe what happens as the longitudinal position of the output slit is changed. As the slit is moved farther away from the back focal plane of the lens ($d_2 > f$), the rays that the slit intercepts are no longer of the same wavelength as illustrated in Fig. 3(a). For large enough displacement of the slit, longer wavelength components at the slit map uniquely to larger spatial displacements at the input. Thus, each spatial feature is mapped to a different wavelength and the shape of the output spectrum is directly proportional to that of the input masking function $m(x')$. If the slit is moved such that it lies within the back focal plane of the lens ($d_2 < f$), the same process occurs, but the sense of the space-to-wavelength mapping is reversed as shown in Fig. 3(b) - rays from larger values of input position are now mapped to shorter wavelengths.

The correspondence between the spatial location of a ray just after the grating (x') and the wavelength for which this ray arrives at a specific output location (x_s) can in fact be calculated from the ray transfer matrix (RTM) [12] of the system (note, here we are no longer assuming that $d_1 = f$)

$$M = \begin{bmatrix} A & B \\ C & D \end{bmatrix} = \begin{bmatrix} 1-\frac{d_2}{f} & \frac{f(d_1+d_2)-d_1d_2}{f} \\ -\frac{1}{f} & 1-\frac{d_1}{f} \end{bmatrix}. \tag{13}$$

From simple geometric optics, the position of a ray at the output (x_s) is

$$x_s = Ax' + B\theta_i, \tag{14}$$

where we take the ray direction θ_i to be the diffraction angle of a wavelength λ relative to the

#5072 - $15.00 US Received 17 August 2004; revised 27 September 2004; accepted 1 October 2004

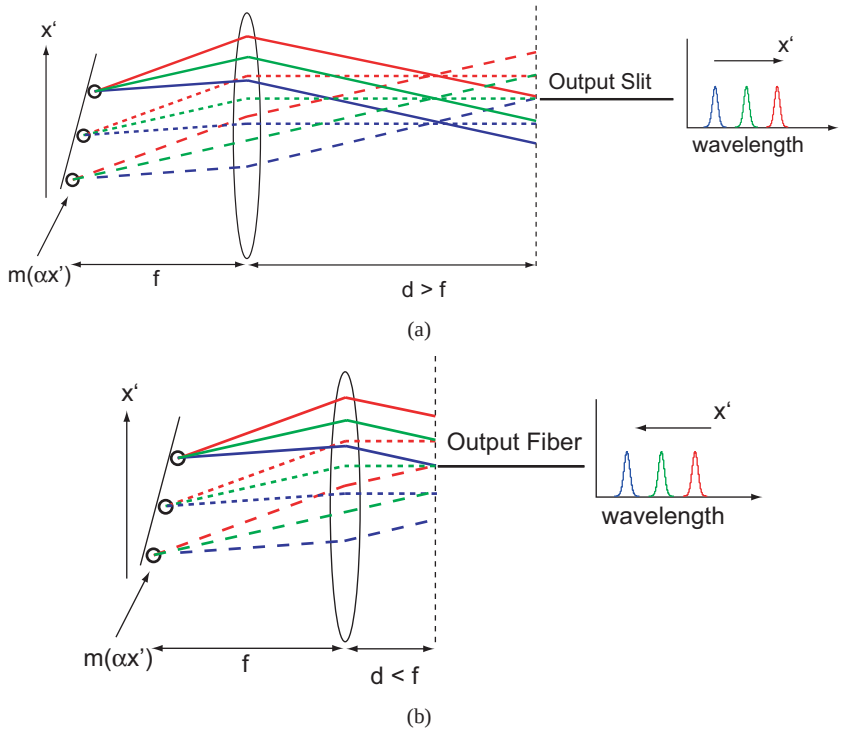

Fig. 3. As the longitudinal position of the output slit is varied, the slit selects different wavelength portions from each input spatial feature. In the spectral domain, each input spatial feature is mapped to a different portion of the optical spectrum. The sense of the mapping from space to time and optical frequency is determined by whether d_2 is greater or less than the focal length f of the spectrometer lens as illustrated in (a) where $d_2 > f$ and (b) where $d_2 < f$.

spectrometer center wavelength λ_o

$$\theta_i \;=\; \theta_D \;=\; (\lambda - \lambda_o)\,\frac{d\theta_D}{d\lambda}. \tag{15}$$

In analogy with equations (10) and (11), we use $\lambda_s(x_s)$ to denote the wavelength for which an input ray at $x' = 0$ arrives at output location x_s. From Eqs. (14) and (15), this gives

$$x_s \;=\; B\,[\lambda_s(x_s) - \lambda_o]\,\frac{d\theta_D}{d\lambda}. \tag{16}$$

Above, the focal length f of the spectrometer lens present in Eq. (10) has been replaced with the effective system length B from the RTM. Now using Eqs. (14), (15), and (16) we find that a ray of wavelength λ arriving at output position x_s must have come from an input position given by

$$x' \;=\; -\,[\lambda - \lambda_s(x_s)]\,\frac{B}{A}\left(\frac{d\theta_D}{d\lambda}\right). \tag{17}$$

In the limit (to be discussed further below) where this ray picture is adequate to predict the spectral passband function, the transmittance of wavelength λ through a thin slit at position x_s

#5072 - $15.00 US Received 17 August 2004; revised 27 September 2004; accepted 1 October 2004

is proportional to the amplitude of a ray at input position x' given by Eq. (17). This amplitude is in turn proportional to $m(\alpha x')$ (through Eq. (4)) where the scale factor α of Eq. (6) accounts for the astigmatism of the grating. Therefore, the field amplitude $E(x_s,\lambda)$ is described by

$$E(x_s,\lambda) \propto m\left\{-[\lambda-\lambda_s(x_s)]\frac{\alpha B}{A}\left(\frac{d\theta_D}{d\lambda}\right)\right\}. \tag{18}$$

We define the space-to-wavelength conversion constant to be

$$\frac{d\tilde{\lambda}}{dx'} = -\frac{A}{\alpha B}\left(\frac{d\theta_D}{d\lambda}\right)^{-1} \quad \left(\frac{\text{nm}}{\text{mm}}\right), \tag{19}$$

where the wavelength offset

$$\tilde{\lambda} = \lambda-\lambda_s(x_s) \tag{20}$$

has been defined to simplify notation. When the spectrometer lens is displaced far enough that this simple picture holds, we can then determine the spectrometer passband function directly by evaluating the applied spatial masking function as a function of wavelength offset from the wavelength $\lambda_s(x_s)$

$$E\left(\tilde{\lambda}\right) \propto m\left[\tilde{\lambda}\left(\frac{d\tilde{\lambda}}{dx'}\right)^{-1}\right]. \tag{21}$$

The same system operation and space-to-wavelength mapping is obtained from a diffraction analysis of the system. It has been shown [13] that the Fresnel integral for a paraxial system can be written directly from the RTM of the system through application of Fermat's principle to the optical path length. This yields the following diffraction integral for our generalized spectrometer (where we have inserted Eq. (4) for $p(x')$)

$$E_{out}(x,\lambda) \propto \int_{-\infty}^{\infty} dx'\, m(\alpha x')\, exp\left(-jk_o\frac{A}{2B}x'^2\right) exp\left(j\xi x'\right). \tag{22}$$

Here we have simplified the notation by defining the wavelength-coupled spatial frequency ξ to be

$$\xi = k_o\left[\frac{x}{B}-(\lambda-\lambda_o)\frac{d\theta_D}{d\lambda}\right]. \tag{23}$$

We are interested in the intensity of the field at the output to our spectrometer, so the phase terms preceding the above integral have been excluded. The above equation is simply the Fourier transform of the applied spatial masking function convolved with a quadratic phase function in the spatial frequency domain,

$$E_{out}(x,\lambda) \propto M\left(\frac{\xi}{\alpha}\right) * exp(j\frac{B}{2k_oA}\xi^2). \tag{24}$$

The spatial chirp rate, defined as the second derivative of the spatial phase in Eq. (22), determines the shape of $E_{out}(x,\lambda)$ above. When the applied masking function is sufficiently slowly-varying (that is, $M(\xi/\alpha)$ is bandlimited) and the lens displacement is large enough that the spatial chirp rate satisfies the condition

$$\left|\frac{d^2\phi(x')}{dx'^2}\right| = \left|k_o\frac{A}{B}\right| \gg \frac{\alpha^2\pi^2}{2\Delta x_{min}^2} \tag{25}$$

#5072 - $15.00 US Received 17 August 2004; revised 27 September 2004; accepted 1 October 2004

for a desired minimum resolvable input feature size Δx_{min} prior to the grating, the convolution [14] may be written as

$$E_{out}(x,\lambda) \propto \int_{-\infty}^{\infty} d\xi' M\left(\frac{\xi'}{\alpha}\right) exp\left(-j\frac{B}{k_o A}\xi'\xi\right). \tag{26}$$

This expression is simply the applied spatial masking function $m(x')$ where the input coordinate x' is now evaluated as a function of output coordinate x and wavelength

$$E_{out}(x,\lambda) \propto m\left\{\frac{\alpha}{A}\left[x - B(\lambda-\lambda_o)\frac{d\theta_D}{d\lambda}\right]\right\}. \tag{27}$$

As a note, the condition of Eq. (25) is equivalent to the condition $(B/2k_oA)\xi_{max} \ll 1$ in [14] and simply ensures that two input spatial features Δx_{min} apart are resolvable in the spatial frequency domain. After sampling the field at the output of the spectrometer in Eq. (27) with a δ-function slit positioned at x_s we have

$$E_{out}(x_s,\lambda) \propto m\left\{\frac{\alpha}{A}\left[x_s - B(\lambda-\lambda_o)\frac{d\theta_D}{d\lambda}\right]\right\}. \tag{28}$$

Using the spatial dispersion of the spectrometer to relate x_s to the passband center wavelength as in Eq. (16), the mapping from location x' and wavelength at the output location x_s is given by

$$x' = -[\lambda - \lambda_s(x_s)]\frac{\alpha B}{A}\left(\frac{d\theta_D}{d\lambda}\right). \tag{29}$$

If we define the wavelength offset $\tilde{\lambda}$ as in Eq. (20), we again obtain the space-to-wavelength conversion constant of Eq. (19)

$$\frac{d\tilde{\lambda}}{dx'} = -\frac{A}{\alpha B}\left(\frac{d\theta_D}{d\lambda}\right)^{-1} \quad \left(\frac{\text{nm}}{\text{mm}}\right).$$

Inserting A and B from the system RTM, $(d\theta_D/d\lambda)^{-1}$, and α the space-to-wavelength conversion constant in terms of the system parameters is given by

$$\frac{d\tilde{\lambda}}{dx'} = -\frac{f-d_2}{f(d_1+d_2)-d_1d_2}\frac{d\cos\theta_D^2}{\cos\theta_i} \quad \left(\frac{\text{nm}}{\text{mm}}\right). \tag{30}$$

We now present several compelling examples of space-to-wavelength mapping in our system.

3. Experiment

Our generalized spectrometer consists of a 600 l/mm low polarization-dependent loss diffraction grating and a 150 mm achromat lens. The output of the spectrometer is sampled with a singlemode optical fiber (mode-field diameter of $\sim 10.5\ \mu$m at 1550 nm). The system center wavelength is nominally $\lambda_o \approx 1550$ nm and the grating is positioned with an incident angle of $\theta_i = 12^\circ$. These result in an astigmatism of $\alpha \approx 1.4$ and a spatial dispersion of $\partial\lambda/\partial x \approx 7.7$ nm/mm, when the apparatus is aligned in an $f-f$ configuration. In this work, the broadband input is an unpolarized, erbium amplified spontaneous emission (ASE) source. The spatial masking functions in this work are periodic spot patterns generated using a diffractive optical element (custom device from INO, Quebec, Canada) which are subsequently manipulated using a series of fixed spatial masks.

#5072 - $15.00 US Received 17 August 2004; revised 27 September 2004; accepted 1 October 2004

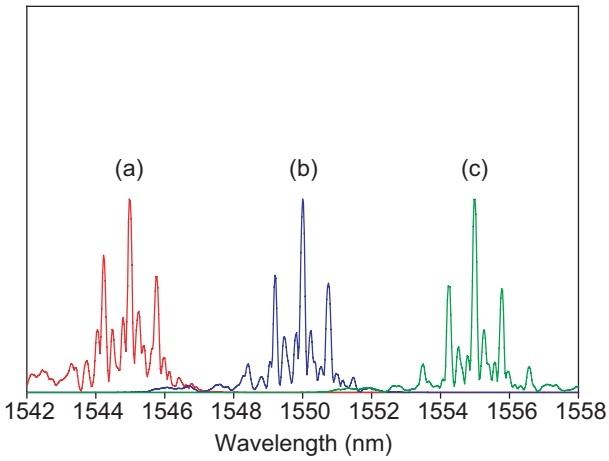

Fig. 4. For a perfectly aligned spectrometer ($d_1 = d_2 = f$ in Fig. 1), the shape of the passband function is related to the Fourier transform of the input masking function. As the transverse position of the output fiber is changed, the passband function center wavelength changes while the overall shape is maintained. Here, the input masking function consists of 10 periodically-spaced spots and the center wavelength is varied from 1545 nm in (a) to 1555 nm in (c). The spatial period of $\sim$3.3 mm corresponds to a modulation of $\sim$0.75 nm ($\sim$94 GHz at λ_o = 1550) as shown by the sidebands in (a) - (c).

When the spectrometer is aligned with the grating-lens and lens-fiber separations equal to the focal length of the spectrometer lens ($d_1 = d_2 = f$), the spectrometer passband function is given by the spatial Fourier transform of the applied input masking function $m(x')$ evaluated as a scaled function of wavelength. The center wavelength of the passband may then be selected via transverse displacement of the output fiber - as expected in a spectrometer - and from DST pulse shaping theory [2], the entire output optical spectrum is repeated about the chosen center wavelength. The spectrometer passband function is measured by dividing the measured output spectrum from the spectrometer by the spectrum of the input ASE source. To illustrate the Fourier transform relation between the input masking function and the measured passband function we apply a periodic 10-spot pattern to the spectrometer input. For this masking function, the $1/e^2$ intensity radius of the spots is approximately 450 μm and the spatial period is nominally 3.3 mm. Figure 4 shows the spectrometer passband function for three output fiber positions. In Fig. 4 (a)-(c) the center wavelength varies over the range of $\sim$ 1540 - 1550 nm, as determined by the transverse output fiber position, while the passband function is found to maintain the same overall highly-structured shape predicted by the Fourier transform of the applied masking function. The irregular shape observed in Fig. 4 (a) - (c) is due to the fact that the DOE imparts different phases to each spot at the input. The sidebands at approximately $\pm$0.75 nm due to the 3.3 mm spatial period at the input are quite clear in all three cases. This clearly demonstrates that when the spectrometer is aligned in an $f - f$ configuration the desired passband function may be tailored through the Fourier transform relation with the applied spatial input pattern. Thus, arbitrary highly-structured passband functions may be designed in a manner similar to temporal waveform design in Fourier transform pulse shaping [15].

We now illustrate direct tailoring of the passband function enabled by the direct mapping from space to wavelength in the generalized spectrometer when the lens is sufficiently displaced from an $f - f$ alignment. Figure 5 shows the predicted (solid line) and measured space-to-wavelength conversion constant as a function of lens distance from the grating for the range

#5072 - $15.00 US Received 17 August 2004; revised 27 September 2004; accepted 1 October 2004

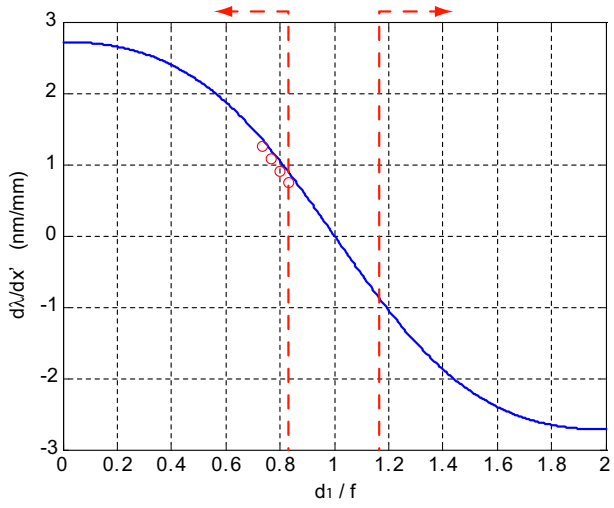

Fig. 5. Space-to-wavelength conversion constant as a function of normalized lens position as calculated from Eq. (30) (solid line) and measured (circles) for our system. The mapping from space to wavelength varies over ∼60% for a total change in lens position of 1.5 cm. The dashed lines show the valid range for the direct scaling assumption ($d_1/f <\sim 0.83$ or $d_1/f >\sim 1.17$) implied by Eq. (25) and the spot spacing of $\Delta x_{min} \approx$3.3 mm of our input patterns.

$0.73f \leq d_1 \leq 0.83f$. The abscissa is the lens distance from the grating normalized to the focal length of the spectrometer lens. In our system, the total distance from the grating to the output fiber is held fixed at twice the focal length of the spectrometer lens; as d_1 varies, d_2 does as well subject to the condition $d_1 + d_2 = 2f$. The space-to-wavelength conversion constant varies by approximately 60% for a change in lens position of only ∼1.5 cm - the result is that the passband function may be scaled by the same amount with very slight changes to the overall system alignment. It is interesting to note the mapping from space to wavelength changes sign about $d_1 = f$. This enables the passband to be reversed about the center wavelength while maintaining the overall spectral scale as alluded to pictorially in Figs. 3(a) and (b).

The dashed lines show the regions of validity for the direct scaling operation ($d_1/f <\sim 0.83$ or $d_1/f >\sim 1.17$). These ranges are determined by the condition of Eq. (25) and the input pattern spot spacing of $\Delta x_{min} \approx$3.3 mm, taking the condition $>>$ in Eq. (25) to be a factor of 5. The upper-bound for the magnitude of the space-to-wavelength conversion constant of $d\tilde{\lambda}/dx' =\sim$ |2.7| nm/mm in Fig. 5 is determined by the fixed grating-fiber separation of $d_1 + d_2 = 2f$ in our apparatus. In general, larger scaling factors could be obtained by removing this constraint thereby allowing d_1 and d_2 to vary independently. Achieving an arbitrarily large linear conversion from space to wavelength as in Eq. (30) is then limited by the physical aperture of the spectrometer components and the validity of the paraxial approximation to the system.

One final note on the range of validity for the direct scaling operation - the condition of Eq. (25) gives one condition for the valid range of operation. The other less obvious point arises when we attempt to achieve a large scaling factor by superposing the grating, lens, and slit ($d_1 = d_2 = 0$). Equation (30) predicts the scaling factor should approach infinity; however, practically there is no spectroscopic action due to the presence of all (positive and negative) diffraction orders. Thus, the direct scaling operation may only be obtained from a single diffraction order

#5072 - $15.00 US Received 17 August 2004; revised 27 September 2004; accepted 1 October 2004

which has been spatially separated from all other orders. In the case of $d_1 = d_2 = 0$, the slit simply samples the transverse intensity of the applied spatial masking function.

We first present scaling of the spectrometer passband function about a fixed center wavelength. The output fiber is positioned in this case to give a center wavelength of ∼1552 nm. The masking function is the same 10-spot pattern used to obtain the highly-structured passband functions of Fig. 4. Figure 6 shows the measured passband function as the lens position (d_1) is varied over the range of 11 cm ($0.73f$) to 12.5 cm ($0.83f$). Here the 10-spot input masking function is clearly mapped to the spectrometer passband. The space to wavelength mapping

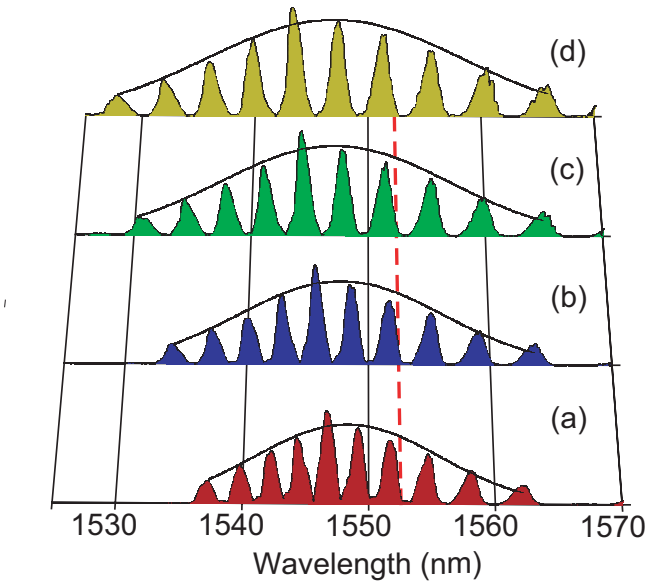

Fig. 6. Spectral scaling properties of the generalized spectrometer. As the spectrometer lens position is varied, the imposed quadratic spatial phase causes the spectrometer passband to be scaled about the center wavelength. In (a)-(d) the measured space-to-wavelength conversion constant and lens distance from the grating (d_1 in Fig. 1) are (a) $d_1 = 12.5$cm, $d\lambda/dx' =\sim 0.74$ nm/mm, (b) $d_1 = 12.0$cm, $d\lambda/dx' =\sim 0.91$ nm/mm, (c) $d_1 = 11.5$cm, $d\lambda/dx' =\sim 1.08$ nm/mm, and (d) $d_1 = 11.0$cm, $d\lambda/dx' =\sim 1.24$ nm/mm. The solid curves are numerical fits to the spectral aperture determined by the mode of the output fiber.

$d\lambda/dx'$ - measured by taking the ratio of difference in peak location in wavelength and difference in spatial spot location at the grating of any two spots - varies from $\sim$ 0.74 nm/mm in Fig. 6(a) to $\sim$ 1.24 nm/mm in Fig. 6(d). These agree reasonably well with the values predicted by Eq. (30) of 0.88 nm/mm in Fig. 6(a) to 1.35 nm/mm in Fig. 6(d). The shape and extent of the measured passband agree quite well with our calculations. Given the spacing between the first and last spots in the applied masking function ($\sim$ 30 mm), the spectral passband (measured from the position of the first and last peaks) may be tuned in extent from $\sim$ 24 nm to over 37 nm, which agrees very well with the predicted range of 22 - 37 nm. Over this range of lens position, the extent of the spectral passband is experimentally found to increase by ∼55% from Fig. 6(a) to Fig. 6(d) which agrees very well with our predictions. Note, the center wavelength is the wavelength which is invariant with respect to changes in scaling. In Fig. 6, this wavelength is shown by the dashed line (∼1552 nm). The mapping from space to wavelength occurs relative to the optical axis - since the center of the 10-spot pattern lies slightly off the optical axis, the pattern appears to shift to the left as the space-to-wavelength scaling is increased.

#5072 - $15.00 US Received 17 August 2004; revised 27 September 2004; accepted 1 October 2004

At this point a comment on the passband shape is in order. Ideally, the passband would exhibit equal-amplitude features given the equal intensity spots applied to the system input. However, the Gaussian roll-off evident in the passbands of Fig. 6 (as well as all subsequent measured passbands) is due to the finite mode-size of the output fiber (the input masking function $m(x')$ is effectively multiplied by the spatial Fourier transform of the assumed Gaussian fiber mode as shown in [3]). This may be equivalently attributed to the acceptance angle of the fiber. To alleviate this spectral aperture effect, a telescope of appropriate magnification could be inserted between the basic spectrometer and the output fiber. This technique effectively broadens the spectral aperture by a factor of the telescope magnification and has previously been demonstrated for increasing the available pulse shaping time aperture of the DST pulse shaper [3]. The measured width of the spectral aperture provides further verification of the space to wavelength mapping. Using Gaussian beam transformations in an $f-f$ configuration, the $w_o = 10.5$ μm $1/e$ mode-field diameter of the fiber transforms to an equivalent

$$16.6 \text{ mm} \;=\; \sqrt{2\ln 2}\,\frac{f\lambda}{\pi w_o} \tag{31}$$

intensity fullwidth half-maximum (FWHM) Gaussian aperture at the grating. The theoretical FWHM spectral aperture (black curves in Fig. 6) is the product of the space-to-wavelength conversion constant and the equivalent spatial aperture at the grating (Eq. (31)). The observed spectral apertures are in good agreement with those predicted using this formulation.

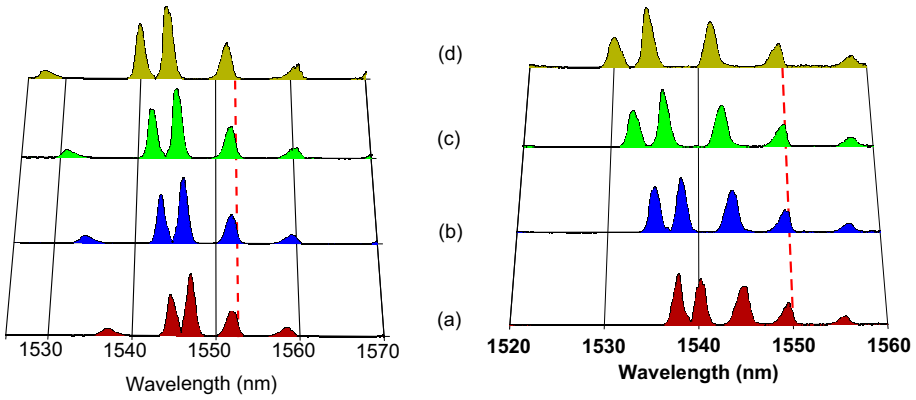

Fig. 7. Scaling of asymmetric spectral passbands about center wavelengths of ∼1552 nm and ∼1550 nm. The lens positions and space-to-wavelength conversion constants correspond to those of Fig. 6 (a) - (d).

Several more examples of passband scaling about center wavelengths (invariant points) of ∼1552 nm and ∼1550 nm are shown in Figure 7. Here, the applied masking functions are no longer symmetric in space and, accordingly, the measured passband functions are asymmetric in wavelength. We note that here, the lens positions in Fig. 7 (a) - (d) correspond to the same positions as in Fig. 6. As a result, the spatial features corresponding to larger x' values at the input are mapped to longer wavelengths. Though not shown here, the passband will reverse in orientation about the center wavelength yet maintain the same scale if the lens is positioned symmetrically about the point $d_1/f = 1$ in Fig. 5, i.e., d_1 is changed to $f - d_1$ while maintaining the condition $d_1 + d_2 = 2f$.

We note this spectral scaling operation is independent of the transverse output fiber position; hence, the center wavelength of the spectrometer passband may be chosen independently of

#5072 - $15.00 US Received 17 August 2004; revised 27 September 2004; accepted 1 October 2004

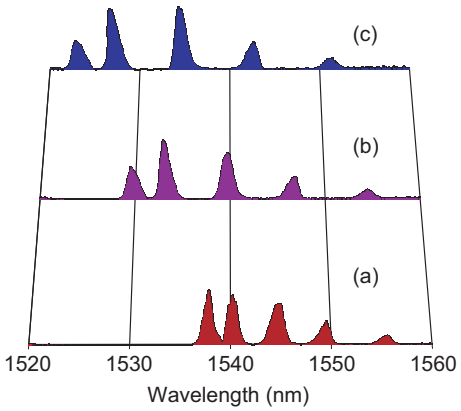

Fig. 8. The passband width and center wavelength may be tuned independently by the spectrometer lens position and output slit position. The space-to-wavelength conversion constant and center wavelength are: (a) $d\lambda/dx' =\sim 0.91$ nm/mm, λ_s=1550.0 nm, (b) $d\lambda/dx' =\sim 1.08$ nm/mm, λ_s=1548.0 nm, and (c) $d\lambda/dx' =\sim 1.24$ nm/mm, λ_s=1544.0 nm.

the passband shape and scale. This is illustrated quite clearly in Figure 8 where the center wavelength is varied from λ_s=1550 nm in Fig. 8(a) to λ_s=1544 nm in Fig. 8(c) as the space-to-wavelength conversion constant is simultaneously varied from $d\lambda/dx \sim 0.91$ nm/mm to $d\lambda/dx \sim 1.24$ nm/mm. This clearly illustrates how the passband function of the spectrometer may be tailored through direct manipulation of the applied spatial masking function.

4. Discussion and conclusion

In conclusion, we present an essentially new method for tailoring of the passband function of a simple diffraction grating-based spectrometer. Spatial patterning of the input beam and translation of the optical components enables generation of highly-structured user defined passband functions which may be scaled and shifted in optical frequency. Through simple changes in the lens or slit longitudinal positions, the relation of the passband to the applied spatial masking function may be tuned from an exact Fourier transform in the case of an $f-f$ alignment to a direct scaling for large lens / slit displacements. This allows broad flexibility in designing the passband function of the generalized spectrometer. The exact limits of the Fourier and direct scaling functionalities of such a system warrant further exploration, as does the transition region between these two regimes.

A few brief comments are in order with respect to the system efficiency and resolution. Regarding the efficiency - as with any spectrometer, when the apparatus' output is sampled with a single thin slit, the system efficiency scales approximately as the ratio of the optical bandwidth accepted by the slit to the total input source bandwidth. For our apparatus and an input source bandwidth of 50 nm, the efficiency is roughly 1 part in 1000 in the direct scaling configuration. The key functionality of the device is the repetitive nature of the passband, i.e., it is repeated at all possible center wavelengths (consider Eqs. (11) and (12)). Thus, if one uses multiple sampling slits, the efficiency increases as the number of slits. Alternatively, the use of a photodetector array at the output not only increases the efficiency, but also provides the full frequency-dependent correlation function between the input spectrum and the spectrometer passband function in a single measurement. This functionality is the primary advantage of our current apparatus over the more widely used Fourier transform (4-f) geometry [15]. Though

#5072 - $15.00 US Received 17 August 2004; revised 27 September 2004; accepted 1 October 2004

the same frequency correlation operation could be achieved in the 4-f configuration using a spatial light modulator (SLM) and detector array for a single frequency, measurement of the full frequency-dependent correlation function could not be achieved in a single shot (the necessary shift of the passband requires reprogramming of the LCM). It is interesting to note as well that the efficiency in the correlating configuration of our generalized spectrometer is virtually the same as it would be for the 4-f configuration, excluding any loss incurred during spatial patterning of the input beam (avoidable using diffractive optics [16] for spatial patterning).

The minimum resolution of the generalized spectrometer - achieved when the apparatus is aligned in an $f-f$ configuration - is essentially the same as that of a spectrometer without a patterned beam. That is, the minimum resolution is inversely proportional to the spatial extent of the beam (or the entire spatial pattern) at the diffraction grating. For our current system, using a 600 l/mm grating, a spatial pattern extent of $\sim$3 cm, and a center wavelength of 1550 nm the minimum resolution is $\sim$.08 nm. The new direct scaling functionality is achieved at the expense of apparatus' resolution. In the direct-scaling configuration, the resolution is no longer determined solely by the pattern size at the grating. The direct-scaling condition of Eq. (25) now sets the minimum input spatial feature size and the space-to-wavelength mapping (Eq. (30)) then determines the corresponding spectral feature size. The difference here is that it is now the spatial extent of a single feature - not the entire pattern - that determines the apparatus' resolution. The input spatial pattern and space-to-wavelength scaling must then be chosen according to the desired system resolution in the direct-scaling configuration.

We note that in addition to gratings, the system functionality can be realized using a variety of spectral dispersers such as prisms or virtually-imaged phased arrays (VIPAs) [17, 18], with the choice determined by the desired scaling range and source bandwidth. Incorporation of programmable spatial masking using spatial light modulators (both one- and two-dimensional) will allow dynamic control over the spectrometer passband and, we believe, lead to novel approaches in the field of correlation spectroscopy as well as ultrafast optical signal processing and broadband spectral imaging.

This work was supported by the U.S. Army Research Office under contract DAAD19-00-0497.

#5072 - $15.00 US Received 17 August 2004; revised 27 September 2004; accepted 1 October 2004